

## Curvature and Charge Modulations in Lamellar DNA–Lipid Complexes

Daniel Harries,<sup>\*,†,‡</sup> Sylvio May,<sup>§</sup> and Avinoam Ben-Shaul<sup>†</sup>

Department of Physical Chemistry and the Fritz Haber Research Center, The Hebrew University, Jerusalem 91904, Israel, and Institute of Molecular Biology, Friedrich-Schiller University, Jena, Winzerlaer Strasse 10, Jena 07745, Germany

Received: July 29, 2002; In Final Form: January 9, 2003

To model the possible formation of coupled spatial corrugations and charge density modulations in lamellar DNA–lipid complexes, we use a free energy functional which includes the electrostatic, lipid mixing, and elastic degrees of freedom in a self-consistent manner. We find that the balance of forces favors membrane corrugations that are expected to be stable with respect to thermal membrane undulations for a certain range of lipid (charged and uncharged) composition. This may lead to locking between DNA strands in adjacent galleries of the complex. Furthermore, the possibility of membrane corrugations renders the lamellar complex more stable with respect to another, hexagonal, DNA–lipid phase.

## 1. Introduction

The condensed complexes formed between DNA and cationic lipids, also known as “lipoplexes”, have attracted much attention in recent years, mainly because of their potential use as nonviral transfection vectors for gene therapy.<sup>1–3</sup> Lipoplexes are formed spontaneously in aqueous solutions upon mixing DNA and liposomal lipid bilayers composed of cationic lipids (CL), electrically neutral, “helper” lipids (HL), and possibly additional molecules such as cholesterol. Detailed structural measurements, primarily X-ray, freeze fracture electron microscopy, and cryo-transmission electron microscopy (cryo-TEM) studies, reveal two major lipoplex geometries: lamellar ( $L_{\alpha}^C$ ) and hexagonal ( $H_{II}^C$ ).<sup>3–8</sup> The lamellar complexes are smectic-like arrays of stacked lipid bilayers with monolayers of DNA molecules, oriented parallel to each other, intercalated within the intervening water gaps. The hexagonal complexes consist of an inverse-hexagonal lipid phase, with DNA “rods” intercalated within their cylindrical aqueous tubes. These hexagonal, or “honeycomb” complexes, may also be depicted as a super-lattice of hexagonally packed “monolayer coated DNA” units. A third (“spaghetti-like”) lipoplex geometry consists of a single (double stranded or supercoiled) DNA enveloped by a lipid bilayer. Theory suggests that this structure is metastable with respect to the hexagonal geometry.<sup>9</sup>

From a physicochemical viewpoint, lipoplex formation provides one of the most striking examples of macroion association in solution, featuring rich and theoretically challenging phase and structural behaviors. For instance, it has been unequivocally demonstrated, both theoretically and experimentally, that the spontaneous association of DNA and CL/HL bilayers is driven by the entropic gain associated with the release into the bulk solution of the counterions previously bound to these, oppositely charged, macroions.<sup>10–12</sup> Consistent with this

conclusion, it was found that the complexes are maximally stable at the *isoelectric point*, where the total surface charges on the DNA and lipid layers are equal in magnitude, enabling perfect charge matching and hence maximal *counterion release*, just as in the interaction between two infinite, oppositely charged planar surfaces.<sup>10,11,13–15</sup>

Lipoplex formation highlights all of the unique properties of lipid membranes, namely, their being *self-assembled* two-dimensional *fluid mixtures*, *flexible* with respect to curvature deformations. These properties are generally coupled to each other. For instance, simultaneous charge-curvature modulations appear to play an important role in the undulation behavior of mixed lipid bilayers.<sup>16</sup> Similarly, this coupling affects the adhesion characteristics of two apposed membranes or a membrane to a surface. Membrane elasticity, fluidity, and self-assembling properties of lipids play a crucial, generally synergistic, role in the interaction between lipid bilayers and biopolymers such as DNA and proteins. For example, the formation of hexagonal lipoplexes from DNA and planar bilayers could only happen because the lipids constituting the bilayer can reassemble in the hexagonal symmetry. The elastic properties of the lipids govern the preferred complex geometry. For instance, it is well-known, and understood, that “soft” lipid bilayers (characterized by small bending rigidity,  $\kappa \approx k_B T$ ) tend to form  $H_{II}^C$  rather than  $L_{\alpha}^C$  complexes, because the former enable better electrostatic matching. The preferred geometry can also be controlled by tuning the spontaneous curvature ( $c_0$ ) of the HL/CL mixture; for example, the helper lipid DOPE (dioleoylphosphatidylethanolamine) possesses negative spontaneous curvature, thus favoring the  $H_{II}^C$  phase.<sup>3,9,17</sup>

Being a 2D *fluid mixture*, the lipid membrane allows its constituent molecules to diffuse within the membrane plane, enabling them to respond to interactions with neighboring macromolecules through *local changes in composition*. In particular, the cationic lipids in the  $L_{\alpha}^C$  complex tend to redistribute in the bilayer plane so as to locally match the charge density on the DNA strands, as illustrated in Figure 1a, and corroborated experimentally.<sup>18</sup> It should be noted that this electrostatically induced modulation in lipid composition is partially inhibited by the concomitant loss of 2D mixing entropy.

\* To whom correspondence should be addressed. E-mail: harries@helix.nih.gov.

† The Hebrew University.

‡ Current address: Laboratory of Physical and Structural Biology, National Institute of Child Health and Human Development, National Institutes of Health, Bethesda, MD, 20892-0924.

§ Friedrich-Schiller University.

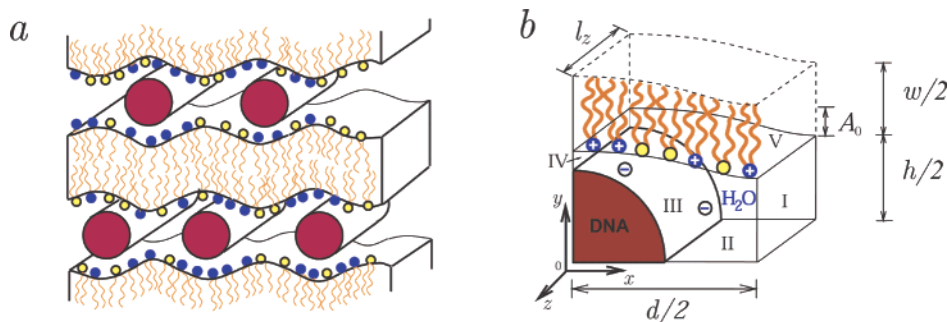


**Figure 1.** (a) Schematic illustration of the lamellar ( $L_{\alpha}^C$ ) lipid-DNA complex. (b) Illustration of the complex (quarter) unit cell.

The ultimate “annealed” composition profile reflects a balance of these opposing tendencies.

As noted above, very “soft” (low  $\kappa$ ) or “curvature-loving” (negative  $c_0$ ) lipid mixtures will typically prefer the high curvature of the hexagonal complex over the planar geometry of the lamellar complex. Moderately soft bilayers ( $\kappa \approx 10k_B T$ ) will generally prefer the planar symmetry of the  $L_{\alpha}^C$  complex but may nevertheless develop sizable curvature modulations, as depicted in Figure 1a. These membrane corrugations provide partial enveloping of the DNA rods by the lipid bilayer (thus improving the electrostatic matching) provided of course that the local change in membrane curvature is “in-phase” with a local variation in membrane charge density. In other words, the *curvature* and *lipid composition* corrugation profiles are intimately coupled to each other and dictated, as usual, by the requirement for a global minimum of the complex’s free energy.

Our goal in this work is 2-fold. First, to show how the coupling between the bilayer’s lipid composition and curvature degrees of freedom is reflected in the interaction free energy of a macroion-membrane system. The second is to examine the consequences of this coupling with respect to the structure, stability and phase behavior of the  $L_{\alpha}^C$  complex. Our approach is based on an extension of a unified theoretical scheme allowing for the explicit inclusion of lipid mobility effects (and hence local demixing) in the electrostatic free energy of membrane-macroion system, such as the  $L_{\alpha}^C$  complex, or a “protein-dressed” membrane.<sup>12,19</sup> Fleck et al.<sup>20</sup> have recently shown that the electrostatic free energy may be further generalized so as to include the effects of ionizable (i.e., not fully ionized) lipid headgroups. In their study, as in our previous work, the lipid bilayers were treated as perfectly planar. In the present work, as we have just stressed, we explicitly allow for curvature modulations.

Membrane corrugation, as schematically illustrated in Figure 1a, suggest the possible appearance of spatial correlations between monolayers of DNA in neighboring “galleries”. Cryo-TEM studies of the  $L_{\alpha}^C$  phase seem to support this notion.<sup>5</sup> Similarly, X-ray measurements clearly indicate correlated curvature-charge corrugation and 3D registry between galleries in an  $L_{\alpha}^C$  complex. However, the lipid layers in this experiments were in their crystalline (“gel”) phase.<sup>21</sup> Further support for the possible appearance of membrane corrugations is provided by computer simulations of the lamellar complex.<sup>22</sup> When the amplitude of membrane corrugation is small, there is no a priori reason for spatial “locking” of DNA monolayers belonging to different galleries. Yet, even in the absence of membrane troughs, DNA rods in adjacent galleries may be correlated with each other through other interaction mechanisms. It is also possible that, while positional correlations between DNA rods in neighboring galleries no longer exist, orientational correlations are preserved. The possible appearance of this rather

special “sliding phase” has attracted considerable theoretical and experimental attention.<sup>23–26</sup> However, no explanation has been provided regarding the molecular origin of the interactions favoring the appearance of such a phase.

The possibility of membrane curvature modulations in an  $L_{\alpha}^C$ -like complex has recently been addressed by Schiessel et al.<sup>27,28</sup> Treating the electrostatic interactions in the linearized (Debye–Hückel) limit of Poisson–Boltzmann (PB) theory, these authors derive scaling relations between the amplitude of membrane curvature undulations, bending rigidity, and surface charge density. Their model does not allow for lipid mobility within the membrane plane, treating the bilayer as a (flexible) surface of uniform charge density and elastic properties. In addition, the membranes are treated as transparent with respect to the electric field. For lipid bilayers of typical bending rigidities ( $\kappa \approx 10k_B T$ ), the amplitudes are found to be quite small, on the order of 1 Å. The authors did not consider the stability of membrane corrugation with respect to thermal curvature fluctuations.

## 2. Theory

We model the  $L_{\alpha}^C$  complex as an ordered array, periodic in the  $x, y$  plane, and translationally invariant along the  $z$  axis, parallel to the axial direction of the DNA molecules (see Figure 1). Suppose there are  $N^+$  cationic lipids,  $N^0$  helper lipids, and  $M$  DNA (phosphate) charges in an arbitrary, large portion of the complex. The structure and free energy of the complex depends on two intensive composition variables, namely, the average mole fraction of charged lipid  $\phi = N^+/(N^+ + N^0)$  and the ratio  $\rho = N^+/M$  between positive (lipid) and negative (DNA) charges. (We assume that the cross sectional areas per CL and HL are equal,  $a$ , so that  $\phi$  is also the area fraction of charged lipid in the bilayer.) All other composition variables are assumed to be fixed, in particular, the salt concentration in the bulk solution (dictating a Debye screening length  $l_D = 10$  Å). In principle, at equilibrium,  $\phi$  and  $\rho$  dictate all of the structural characteristics of the complex, such as the interaxial distance between neighboring DNA molecules,  $d$ , the interbilayer distance,  $h$ , and the thickness of the lipid bilayers,  $w$ . Ignoring the electrostatic coupling between charged surfaces belonging to the same bilayer,  $w$  does not enter our model. This assumption holds when  $\epsilon_{oil}/\epsilon_{water} \ll w/l_D$  with  $\epsilon_{oil} \approx 2$  and  $\epsilon_{water} \approx 80$  denoting the dielectric constants within the hydrophobic (“oily”) interior of the membrane and the aqueous solution, respectively.<sup>29</sup> Typically,  $l_D \approx 10$  Å and  $w \approx 40$  Å, ensuring the fulfillment of the above inequality. Note, however, that the bilayer thickness plays an important role in determining the bending rigidity  $\kappa$ . Finally, both experimentally<sup>7</sup> and theoretically<sup>12</sup> it was shown that the thickness of the water gap,  $h$ , is essentially independent of  $\phi$ , for all relevant compositions. Consistent with this finding, we shall use  $h = 26$  Å, thus setting

the DNA–membrane minimal distance to 3 Å, corresponding to the thickness of the thin hydration layer separating the lipid and DNA charges, (the diameter of double-stranded DNA is  $\approx 20$  Å). The DNA molecules are modeled as cylindrical rods with a radius  $R = 10$  Å. We assume DNA (double) strands to be uniformly charged on their surface with a charge density  $\sigma^- = e/2\pi Rl \approx 0.15\text{Cm}^{-2}$ , corresponding to an average distance between charges along the B-DNA axis of  $l = 1.7$  Å, with  $e$  denoting the elementary charge. The validity of this approximation has previously been discussed.<sup>12,15</sup>

We assume that prior to complex formation the lipid bilayer is symmetric (comprised of two identical leaflets) and therefore planar. Furthermore, the two-dimensional (2D) lipid mixture is assumed to behave ideally. Upon complex formation with DNA, neither the uniform lipid composition nor the planarity of the membrane are preserved. From the symmetry of the complex in Figure 1, it follows that both the local composition and curvature profiles are functions of  $x$ . Hereafter, we shall define a unit cell of the complex as the region of dimensions  $d \times h \times l_z$ , encompassing the region bounded between two adjacent DNA strands ( $d$  along  $x$ ) and two apposed bilayers ( $h_0$  along  $y$ ), and an arbitrary length along the  $z$  axis which later, in the numerical calculations, we set to  $l_z = 1$  Å. The composition and curvature profiles, defined within the unit cell, will be denoted by  $\eta(x)$  and  $c(x)$ , respectively. The curvature profile is equivalently specified by  $h(x)$  the local distance between the surfaces of apposed bilayers. All of our calculations are performed per unit cell of the complex, implying that we cannot account for modulations of length scale larger than  $d$  which, we believe, are totally irrelevant. Another convenient structural characteristic is the contour length,  $l_m$ , along the membrane interface, extending from one DNA to the next;  $l_m \geq d$ , with the equality holding for a perfectly planar complex. Because  $l_m$  is proportional to the number of lipid molecules within a unit cell, it is a constant with respect to variations in  $c(x)$  and is therefore convenient computationally.

Using  $f_c = f_c(\phi, l_m, h)$  to denote the free energy per unit cell, we express this functional as a sum of four terms

$$\begin{aligned}
 f_c = & \int_V \frac{\epsilon}{2} (\nabla\psi)^2 dv \\
 & + k_B T \int_V \left[ n_+ \ln \frac{n_+}{n_0} + n_- \ln \frac{n_-}{n_0} - (n_+ + n_- - 2n_0) \right] dv \\
 & + \frac{k_B T}{a} \int_s \left[ \eta \ln \frac{\eta}{\phi} + (1 - \eta) \ln \frac{1 - \eta}{1 - \phi} \right] ds \\
 & + \frac{1}{2} \int_s \kappa (c - c_0(\eta))^2 ds \quad (1)
 \end{aligned}$$

The first term here is the electrostatic energy, with  $\epsilon$  denoting the dielectric constant of water;  $\epsilon = \epsilon_0\epsilon_r$ , and we shall assume  $\epsilon_r = 78$ , whereas  $\epsilon_0$  is the permittivity of vacuum. The reduced electrostatic potential is  $\psi = e\varphi/k_B T$ ,  $k_B$  is Boltzmann's constant,  $T$  is the temperature, and  $\varphi = \varphi(x, y)$  is the local value of the electrostatic potential. The second term accounts for the translational ("mixing") entropy of the mobile ions in the complex interior, relative to their entropy in the bulk solution, with  $n_{\pm} = n_{\pm}(x, y)$  denoting the local concentrations of the mobile electrolyte ions and  $n_0$  their bulk concentration (we assume a 1:1 electrolyte). The integration in the first two terms extends over the volume of the unit cell. The third term accounts for the local mixing entropy of charged and neutral lipids in

the membrane plane, with the integration extending over the membrane surface. Locally, i.e., at any  $x$ , the lipids are assumed to be ideally mixed,  $\eta = \eta(x)$  denoting the local composition. The local lipid composition must satisfy the conservation constraint:  $l_m \phi = \int_s \eta ds$ .

The free energy functional consisting of the first three terms has already been applied in a comprehensive analysis of the perfectly planar  $L_{\alpha}^C$  complex,<sup>12</sup> as well as in the study of protein adsorption.<sup>19</sup> The fourth term in eq 1 is new, accounting for the curvature deformation energy of the (locally) cylindrically bent lipid monolayers. We assume that the bending rigidity of the mixed layer,  $\kappa$ , is the same for pure CL and HL layers and is thus also independent of the CL/HL ratio. This assumption is most reasonable for lipids of similar chain length. On the other hand, the spontaneous curvature  $c_0$  is generally rather sensitive to the nature of both the tail and the head of the lipid constituents and is thus a more sensitive function of the lipid composition. Following previous analysis, we use the linear interpolation dependence<sup>30,31</sup>  $c_0(\eta) = c_0^c + \eta(c_0^c - c_0^h)$ , where  $c_0^c$  and  $c_0^h$  are the spontaneous curvatures of the cationic and helper lipids, respectively.

The equilibrium characteristics of the complex, including the membrane and composition profiles and its free energy, are determined, for any given  $\phi$ ,  $h$ , and  $d$  (or  $l_m$ ), by the simultaneous minimization of  $f_c$  with respect to  $n_{\pm}(x, y)$ ,  $\eta(x)$  and  $h(x)$  (or  $c(x)$ ) subject to the charge conservation condition  $\int \eta(x) dx = l_m \phi$ . Although possible, this multidimensional minimization yields a set of equations whose numerical solution is quite impractical. We shall thus adopt a somewhat less general, yet similarly informative, procedure and determine the equilibrium  $f_c$  in two stages. We shall first minimize  $f_c$  for a given curvature profile  $h(x)$  and then optimize it with respect to  $h(x)$ . The first minimization step yields the usual Boltzmann distributions for  $n_{\pm}(x, y)$ , which upon substitution into Poisson's equation yield the PB equation

$$l_D^{-2} \nabla^2 \psi = \sinh \psi \quad (2)$$

with  $l_D = (\epsilon_0 \epsilon_r k_B T / 2n_0 e^2)^{1/2}$  denoting the Debye screening length. The minimization (with respect to  $\eta(x)$ ) yields the additional equation

$$\ln \frac{\phi(1 - \eta)}{\eta(1 - \phi)} - \psi_s - \lambda = \kappa \{ c - [c_0^c \eta + c_0^h (1 - \eta)] \} (c_0^c - c_0^h) \quad (3)$$

where  $\lambda$  is the Lagrange multiplier conjugate to the charge conservation constraint and  $\psi_s$  is the reduced potential at the membrane surface. Equation 3 may also be regarded as the condition for constant electro-chemical potential of the charged lipid (here given by  $\lambda$ ) everywhere in the membrane. This equation, together with Gauss' law

$$\sigma^+(x) = - \frac{\epsilon k_B T}{e} \nabla \psi_s \cdot \hat{\mathbf{n}} \quad (4)$$

represents the boundary condition for the electrostatic potential on the membrane surface (boundary V in Figure 1b) for a surface with charge density  $\sigma^+(x) = e\eta(x)/a$ . In eq 4,  $\hat{\mathbf{n}}$  is the unit vector normal to the boundary (pointing into the dielectric medium). Equations 2–4 must be solved self-consistently, yielding the electrostatic potential and the composition profile corresponding to the prescribed curvature profile. The other boundary conditions (pertaining to I–IV in Figure 1b) are standard, as in ref 12.

The next stage involves the determination of the curvature profile,  $h(x)$ . In principle, one could perform a general shape minimization, expressing  $h(x)$  as a Fourier sum and evaluating the amplitudes of different wavelength membrane undulations. In the  $L_\alpha^C$  complex, the interaxial, DNA–DNA, distance sets the natural wavelength in the problem equal to  $d$ . We shall thus ignore contributions from any other wavelength and express  $h(x)$  as

$$h(x) = \frac{1}{2}A_0 \cos(2\pi x/d) + h_0 \quad (5)$$

and determine the optimal amplitude of membrane corrugation,  $A_0$ , by minimizing  $f_c$ . Recall that  $h_0 = h(x=0) - A_0 = 26 \text{ \AA}$  is the interlamellar spacing in the planar complex.

The numerical procedure for solving the PB equation<sup>32–34</sup> and for evaluating  $\lambda, \psi$  has been described in previous work.<sup>12</sup> We note that the validity of this mean field approach has also been extensively discussed elsewhere.<sup>12,15</sup>

Membrane surface corrugation, i.e., periodic curvature deformations, can lead to registry between DNA monolayers in different galleries, provided their amplitude is larger than those of thermal membrane undulations. In determining the extent of thermal membrane undulations, we follow the ideal gas analogy of Helfrich and Servuss for the steric interaction in the lamellar phase of lipids.<sup>35,36</sup> In terms of the Monge representation,  $u(x, z)$  gives the vertical displacement of the surface from a plane reference state. The amplitude of membrane thermal fluctuations depends on the material constant  $\kappa$  but also on the area of the undulating membrane patch. For a membrane patch of area  $L_d^2$ , the mean square displacement of membrane height due to thermal fluctuations (of a tensionless membrane) is  $\langle u^2 \rangle^{1/2} = (k_B T / 4\pi^3 \kappa)^{1/2} L_d$ . Melting of 3D order in the lamellar complex is expected to take place when the thermal undulations corresponding to a membrane patch of area  $L_d^2 \approx d^2$  are on the order of the membrane corrugation amplitude  $A_0$ . Thus, registry between galleries is expected when

$$A_0 > \sqrt{\frac{k_B T}{4\pi^3 \kappa}} d \quad (6)$$

### 3. Results

**3.1. Free Energy.** The effect of membrane corrugation on the complex free energy is greatest when the membrane rigidity is small, so that the membrane can adjust its geometry to fit the apposed DNA molecule, achieving better electrostatic contact, at a relatively small elastic energy cost. Figure 2a shows the complex free energy  $f_c$  as a function of membrane composition  $\phi$ , for a soft membrane whose (monolayer) bending modulus for both lipids is  $\kappa = 1k_B T$ , and spontaneous HL and CL curvatures are  $c_0^h = c_0^c = 0$ . All results are shown for 1  $\text{\AA}$  length of DNA. The complex free energy  $f_c$  is shown as a function of membrane composition  $\phi$ , for three values of  $l_m$ . For comparison, we show  $f_c$  for a complex in which the membrane is kept planar.

As has previously been shown,<sup>12</sup> in all cases, a minimum in the free energy is found, corresponding closely to the isoelectric point of the complex. Moreover, we find that the difference between a complex with relaxed (corrugated) membranes and a complex with constrained (uncorrugated-planar) membrane is always largest at the isoelectric point. Close to the isoelectric point, most of the counterions are already released into the bulk solution. Therefore, further gain in free energy can only be achieved by better charge and spatial matching of the apposed

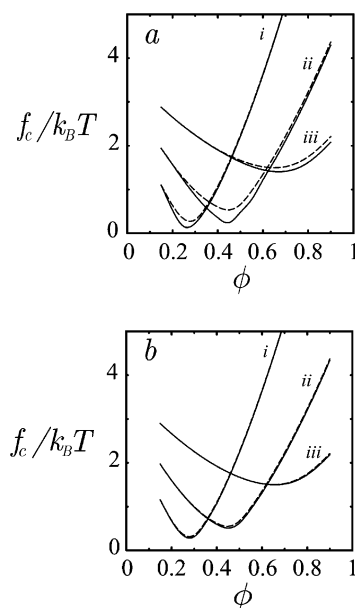


**Figure 2.** Free energy of  $L_\alpha^C$  complex as a function of  $\phi$  for  $l_m = 73 \text{ \AA}$  (i),  $43 \text{ \AA}$  (ii),  $23 \text{ \AA}$  (iii). In a,  $\kappa = 1k_B T$  and  $c_0^h = c_0^c = 0$ ; (b)  $\kappa = 10k_B T$ ,  $c_0^h = 1/100 \text{ \AA}$ , and  $c_0^c = 0$ . The full line corresponds to the corrugated complex, whereas the dashed line to the fully planar one. All energies are given per 1  $\text{\AA}$  length of DNA.

surfaces to optimize the electrostatic interaction energy. Thus, at the isoelectric point, the effect of corrugation (i.e., better fitting of apposed surfaces) on the complex free energy is most substantial. The largest gain in free energy due to corrugations is  $\approx 0.25k_B T$ . The gain from this added degree of freedom for a unit cell the size of DNA's persistence length,  $l_p \approx 50 \text{ nm}$ , is therefore rather large ( $\approx 125k_B T$ ).

When more rigid membranes form complexes, the gain in electrostatic energy is expected to be much smaller, because the penalty for bending is large; the membranes bend only slightly, and consequently, the free energy is not substantially changed. Figure 2b shows the complex free energy as a function of membrane composition  $\phi$ , for membranes with  $\kappa = 10k_B T$  and for the same values of  $l_m$  as in Figure 2a. Here we choose  $c_0^h = 1/100 \text{ \AA}$ ,  $c_0^c = 0$ , modeling a mixture of, e.g., DOPC (dioleoylphosphatidylcholin) and DOTAP (dioleoyltrimethylammonium propane). The gain in free energy following corrugation is only  $\approx 5k_B T$  for a unit cell of length  $l_p$ . Similar results were obtained for membranes where the bending rigidity was  $\kappa = 10k_B T$  and  $c_0^c = 0$ , as before, but with  $c_0^h = -1/25 \text{ \AA}$  (close to the elastic constants measured for DOPE<sup>37–39</sup>).

Allowing for  $L_\alpha^C$  complex corrugation adds somewhat to its stability as compared with the  $H_{II}^C$  phase. Figure 3 shows the complex free energy as a function of membrane composition,  $\phi$ , for soft lipid membranes ( $\kappa = 1k_B T$ ) and  $l_m = 58 \text{ \AA}$  (for which the isoelectric point is at  $\phi \approx 0.35$ ). For comparison, we show the free energy of a complex where corrugations are suppressed and the membranes are flat. In addition, we show the free energy of the competing  $H_{II}^C$  phase for the same number of lipids as in the  $L_\alpha^C$  phase. The free energy for this phase has previously been derived using a similar model to that presented here for the  $L_\alpha^C$  complex, including the elastic, electrostatic, and lipid demixing degrees of freedom.<sup>9,15</sup> Because, in general, the spatial corrugations lower the free energy of the lamellar complex, we can expect spatial modulations to play a role in stabilizing the  $L_\alpha^C$  phase with respect to the  $H_{II}^C$  phase. This is reflected in the values of  $\phi$  at which the free energy curves for the  $L_\alpha^C$  and  $H_{II}^C$  cross when corrugations are allowed

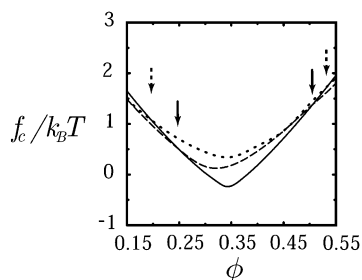


**Figure 3.**  $L_{\alpha}^C$  complex free energy as a function of  $\phi$  for  $l_m = 58 \text{ \AA}$  with allowed corrugations (dashed) and suppressed corrugations (dotted). Also shown is the free energy of the hexagonal complex for the same amount of lipid (full line). In all cases,  $\kappa = 1k_B T$  and  $c_0^h = c_0^c = 0$ . The arrows mark the points of intersection between the free energy of the lamellar and hexagonal complexes.

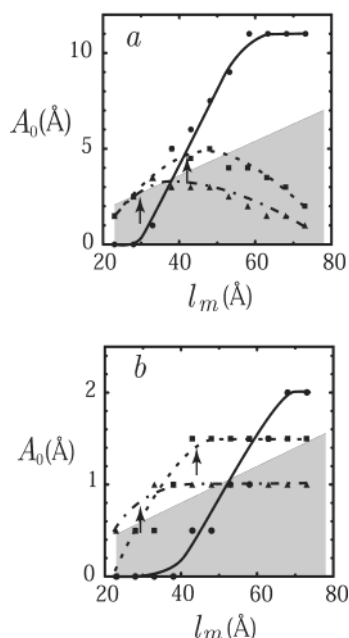


**Figure 4.**  $A_0$  as a function of  $l_m$  for (a)  $\kappa = 1k_B T$  and  $c_0^h = c_0^c = 0$ ; (b)  $\kappa = 10k_B T$ ,  $c_0^h = 1/100 \text{ \AA}$  and  $c_0^c = 0$ . In a and b, the three curves correspond to:  $\phi = 0.25$  (full),  $0.5$  (dotted), and  $0.7$  (dash-dotted). The unshaded area corresponds to eq 4. In all cases, the calculated values are designated by full symbols. The lines are guides for the eye. The arrows indicate the isoelectric point for each curve.

and when they are forbidden. The region along  $\phi$  for which the hexagonal complex is more stable than the lamellar one is narrower for the corrugated complex. We expect the phase boundary to follow this trend as well. The region for which the hexagonal complex will be found to be stable is expected to prevail for a more limited range of  $\phi$ 's.

**3.2. Corrugation Amplitude.** Next we consider the corrugation amplitude as determined from minimizing the free energy. We first consider a soft membrane,  $\kappa = 1k_B T$ , with  $c_0^h = c_0^c = 0$ . The extent of corrugation at equilibrium,  $A_0$ , as a function  $l_m$  for several values of  $\phi$  is shown in Figure 4a. The unshaded area corresponds to the range given by eq 4, representing corrugations that are stable with respect to thermal undulations.

The maximal corrugation occurs for membranes of low  $\phi$ . When the membrane is of low charge (hence high mismatch with the DNA's charge density  $\sigma^- \approx 0.6e/a$ ), the proper matching of the DNA molecule and membrane becomes more important for obtaining maximal counterion release. This matching can be achieved both by charge density modulations and by corrugations. Therefore, we can expect that, if the cost of bending is not too great, the highest modulation will be

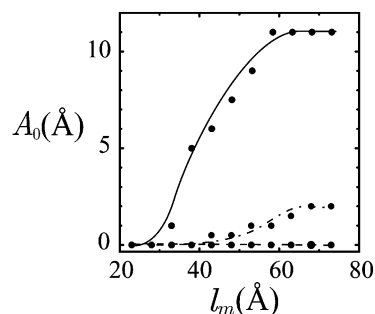


**Figure 5.**  $A_0$  as a function of  $l_m$  for  $\phi = 0.25$ . The three curves correspond to  $\kappa = 1k_B T$ ,  $c_0^h = c_0^c = 0$  (solid line);  $\kappa = 10k_B T$ ,  $c_0^h = 1/100 \text{ \AA}$ , and  $c_0^c = 0$  (dash-dotted);  $\kappa = 10k_B T$ ,  $c_0^h = -1/25 \text{ \AA}$ , and  $c_0^c = 0$  (dashed). In all cases, the calculated values are designated by full symbols. The lines are guides for the eye.

observed for the membrane of lower  $\phi$ . In all cases, a maximum in the corrugation is found at a certain  $l_m$ . This  $l_m$  closely (but not exactly) matches the isoelectric point. At the isoelectric point, the proper release of counterions to solution ultimately depends on the geometrical fit between macroions. It is also clear from Figure 4a that a substantial corrugation is expected for only a limited intermediate range of  $l_m$ 's, for which the corrugation is higher than the expected membrane thermal undulations.

We next consider a more rigid membrane,  $\kappa = 10k_B T$ , with  $c_0^h = 1/100 \text{ \AA}$  and  $c_0^c = 0$ . Figure 4b shows the extent of corrugation,  $A_0$ , as a function  $l_m$  for the same  $\phi$  values as shown in Figure 4a. Again, the unshaded area corresponds to the inequality in eq 4. As expected, for all values of  $\phi$ ,  $A_0$  is smaller than for the soft membranes. The maxima are somewhat shifted to higher  $l_m$  values. This can be easily understood. Because  $\kappa$  is substantially higher, the elastic deformation energy cost is higher. When  $l_m$  is larger, the (average) curvature is smaller for a certain  $A_0$ . It follows that the membranes can deform at a relatively lower energy cost when  $l_m$  is larger. Again, it can be seen that even when the membranes are stiff, stable corrugations may persist for a certain  $l_m$  range. This is due to the fact that both the thermal undulations and the corrugations are smaller for membranes of higher  $\kappa$ . These two effects compensate each other to a large extent.

A clear demonstration of the importance of the elastic contribution to the modulation is a comparison of three different membranes, all with the same  $\phi = 0.25$ . In Figure 5, three membrane types are compared, a soft membrane ( $\kappa = 1k_B T$ ,  $c_0^h = c_0^c = 0$ ), a more rigid membrane with two lipid types of (nearly) vanishing spontaneous curvature ( $\kappa = 10k_B T$ ,  $c_0^h = 1/100 \text{ \AA}$  and  $c_0^c = 0$ ) and a similarly rigid membrane with a HL characterized by a high negative spontaneous curvature ( $\kappa = 10k_B T$ ,  $c_0^h = -1/25 \text{ \AA}$ , and  $c_0^c = 0$ ).

Because the membranes corresponding to the three cases in Figure 5 bear a rather small charge density ( $\phi = 0.25$ ), the effect of the uncharged lipid species is considerable. For membranes of a small bending rigidity, the modulation will be large, as expected. More complex is the case where the bending rigidity is non negligible ( $\kappa = 10k_B T$ ). In this case, there is a pivotal role to the spontaneous curvature of the lipid species. As can be seen, in the case where the HL has a high negative curvature ( $c_0^h = -1/25 \text{ \AA}$ ), the corrugation is suppressed completely (for  $\phi = 0.25$ ), whereas it is substantial ( $A_0 \approx 2 \text{ \AA}$ ) when the HL has a spontaneous curvature of  $c_0^h = 1/100 \text{ \AA}$ . The qualitative reason is as follows. Because charged lipids tend to migrate toward the interaction zone with the DNA, the uncharged lipids

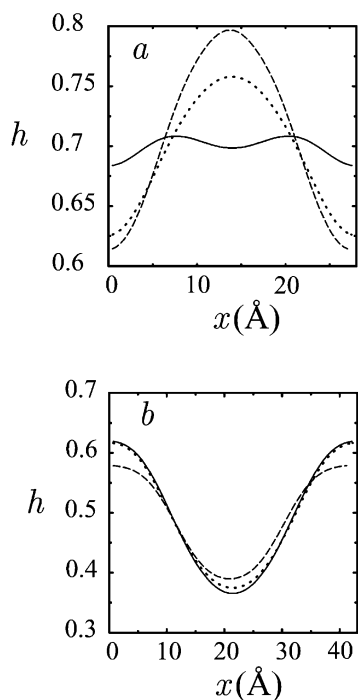


**Figure 6.**  $\eta$  as a function of  $x$  for (a)  $\phi = 0.7$  and  $l_m = 28 \text{ \AA}$ ; (b)  $\phi = 0.5$  and  $l_m = 43 \text{ \AA}$ . In a and b, the three curves correspond to  $\kappa = 1k_B T$ ,  $c_0^h = c_0^c = 0$  (dashed);  $\kappa = 10k_B T$ ,  $c_0^h = 1/100 \text{ \AA}$ , and  $c_0^c = 0$  (solid);  $\kappa = 10k_B T$ ,  $c_0^h = -1/25 \text{ \AA}$ , and  $c_0^c = 0$  (dotted).

are expelled to the region outside the interaction zone. However, the monolayer area outside the interaction zone is of *positive* curvature, so that placing a HL with a negative spontaneous curvature in that region is unfavorable. Ultimately, the system tends to suppress corrugations when the spontaneous curvature of the HL is highly negative, and the bending rigidity is substantial.

**3.3. Charge Density Modulations.** It has previously been shown that charge density modulations can contribute substantially to lowering the complex's free energy.<sup>12</sup> Here, charge and curvature modulations are strongly coupled to each other. This is because each lipid species has combined elastic (bending and spontaneous curvature) and electrostatic (charged or uncharged) properties. At equilibrium, the lipid arrangement (corrugation and charge density modulation) will be determined by the optimum of the free energy.

Figure 6a shows the charge density modulation  $\eta$  as a function of the  $x$  coordinate between two adjacent DNA molecules in the same gallery for a rather small membrane length,  $l_m = 28 \text{ \AA}$  and  $\phi = 0.7$  (very close to the isoelectric point). The modulations are shown for three different membranes, corresponding to the ones in the previous section. In general, the trend toward charge matching on the DNA and membrane is observed (recall  $\sigma^- \approx 0.6e/a$ ) at the point of closest approach between the membrane and DNA molecules (i.e., at  $x = 0$  and  $x \approx 28 \text{ \AA}$ ). At this distance, the effect of the electrostatic interaction is strongest. Thus, charge matching of apposed layers is most effective at this point, enabling a maximal number of counterions to be released from the gap.

The charge density modulation is largest when the membranes are most soft, which also corresponds to the case of largest corrugation. In this case, the importance of charge matching (hence lowering of the disjoining pressure) is greatest, since the membrane is wrapped more tightly around the DNA ( $A_0 \approx 2.5 \text{ \AA}$  for the soft membranes vs  $A_0 \approx 0.5 \text{ \AA}$  for the stiff membranes).

More intricate is the case for complexes formed of rather stiff membranes ( $\kappa = 10k_B T$ ), where the uncharged lipid molecules have a positive spontaneous curvature ( $c_0^h = 1/100 \text{ \AA}$ ). For these, we find that the charge density modulations do not come to a maximum at the point farthest from the interaction zone, i.e., at the midplane between DNA molecules (solid line in Figure 6a). In general, when membranes are stiff, the elastic contribution to the free energy becomes more dominant. Furthermore, in this case, the uncharged lipid molecules possess a (rather low) positive spontaneous curvature, so that elastically it favors the midplane, away from the DNA. However, the same (neutral) lipid species also tends to be drawn *toward* the DNA molecule in order to achieve better electrostatic charge matching between the DNA and membrane (at a certain elastic penalty). The optimum of the two contributions, electrostatic and elastic, which in this case tend to oppose each other, tends to suppress the charge density modulation. The results show that maximum charge density is found where the membrane is *most flat*, reflecting  $c_0^c = 0$ . The uncharged species resides both in the negatively curved region (i.e., favorable electrostatic interaction, unfavorable elastic penalty) and in the positively curved area close to the midplane (i.e., favorable elastic interaction, unfavorable electrostatic interaction).

When  $l_m$  is larger, the resulting modulation is somewhat less complex. Figure 6b shows the charge density modulations for the same three membrane types as before. This time  $\phi = 0.5$  and  $l_m = 43 \text{ \AA}$ , closely corresponding to the isoelectric point.

The charge density modulations are smallest for soft membranes, where corrugations are also more prominent. Charge matching, again, plays an important role in determining the charge density in the proximity of the DNA. Because the wrapping of membrane around DNA for a substantial length of  $x$  implies a larger interaction zone between DNA and lipid, a larger region is expected to fulfill the charge matching tendency, and thus the change in charge density is the smallest.

When the membranes are more rigid, i.e.,  $\kappa = 10k_B T$ , the spontaneous curvature of the HL becomes more important in determining the charge density modulations. Figure 6b reveals that the modulations are largest for  $c_0^h = 1/100 \text{ \AA}$ . For this case, both the electrostatic and elastic considerations to lowering the free energy coincide. While the helper lipid is expected to be (electrostatically) expelled from the interaction zone between DNA and lipid, it also has a (small) positive spontaneous curvature, which matches the curvature of the noninteracting region, i.e., close to the midplane.

#### 4. Concluding Remarks

In this study, we demonstrated the importance of the coupling between curvature deformation, lipid composition, and ensuing surface charge density. This coupling is particularly significant when considering the interaction of fluid lipid membranes with apposed (charged) macromolecules such as proteins and DNA. The approach we use here for determining the free energy enables us to take into account this coupling in a self-consistent manner. For the system of interacting DNA and mixed lipid bilayers, we predict that the curvature and electrostatic contributions to the free energy will favor the formation of corrugated  $L_\alpha^C$  complexes. Not surprisingly, the corrugations are predicted to be particularly large when the membranes are soft (yet not soft enough so as to favor the  $H_{II}^C$  phase). Furthermore, we find that the maximal corrugation can be found close to (but not exactly) at the isoelectric point. Our results suggest that these corrugations could be stable with respect to thermal undulations

for a certain range of membrane compositions and DNA/Lipid ratio. This may lead to a locking of DNA strands in adjacent galleries.

**Acknowledgment.** We thank the Israel Science Foundation, US-Israel Binational Science Foundation and Minerva Society for financial support. S.M. thanks TMWFK.

### References and Notes

- (1) Felgner, P. L. *Sci. Am.* **1997**, *276*, 86–90.
- (2) Barenholz, Y. *Curr. Opin. Colloid Interface Sci.* **2001**, *6*, 66–77.
- (3) Safinya, C. R. *Curr. Op. Struct. Biol.* **2001**, *11*, 440–448.
- (4) Sternberg, B.; Sorgi, F. L.; Huang, L. *FEBS Lett.* **1994**, *356*, 361–366.
- (5) Battersby, B. J.; Grimm, R.; Hübner, S.; Cevc, G. *Biophys. Biochim. Acta* **1998**, *1372*, 379–383.
- (6) Simberg, D.; Danino, D.; Talmon, Y.; Minsky, A.; Ferrari, M. E.; Wheeler, C. J.; Barenholz, Y. *J. Biol. Chem.* **2001**, *276*, 47453–47459.
- (7) Rädler, J. O.; Koltover, I.; Salditt, T.; Safinya, C. R. *Science* **1997**, *275*, 810–814.
- (8) Koltover, I.; Salditt, T.; Rädler, J. O.; Safinya, C. R. *Science* **1998**, *281*, 78–81.
- (9) May, S.; Ben-Shaul, A. *Biophys. J.* **1997**, *73*, 2427–2440.
- (10) Bruinsma, R. *Eur. Phys. J. B* **1998**, *4*, 75–88.
- (11) Wagner, K.; Harries, D.; May, S.; Kahl, V.; Rädler, J. O.; Ben-Shaul, A. *Langmuir* **2000**, *16*, 303–306.
- (12) Harries, D.; May, S.; Gelbart, W. M.; Ben-Shaul, A. *Biophys. J.* **1998**, *75*, 159–173.
- (13) Record, J. M. T.; Anderson, C. F.; Lohman, T. M. *Q. Rev. Biophys.* **1978**, *11*, 103–178.
- (14) Parsegian, V. A.; Gingell, D. *Biophys. J.* **1972**, *12*, 1192–1204.
- (15) May, S.; Harries, D.; Ben-Shaul, A. *Biophys. J.* **2000**, *78*, 1681–1697.
- (16) Guttman, G. D.; Andelman, D. *J. Phys. II (France)* **1993**, *3*, 1411–1425.
- (17) Dan, N. *Biochim. Biophys. Acta* **1998**, *1369*, 34–38.
- (18) Mitrakos, P.; Macdonald, P. M. *Biochemistry* **1996**, *35*, 16714–16722.
- (19) May, S.; Harries, D.; Ben-Shaul, A. *Biophys. J.* **2000**, *79*, 1747–1760.
- (20) Fleck, C.; Netz, R. R.; von Grunberg, H. H. *Biophys. J.* **2002**, *82*, 76–92.
- (21) Artzner, F.; Zantl, R.; Rapp, G.; Rädler, J. *Phys. Rev. Lett.* **1998**, *81*, 5015–5018.
- (22) Bandyopadhyay, S.; Tarek, M.; Klein, M. L. *J. Phys. Chem. B* **1999**, *103*, 10075–10080.
- (23) O'Hern, C. S.; Lubensky, T. C. *Phys. Rev. Lett.* **1998**, *80*, 4345–4348.
- (24) O'Hern, C. S.; Lubensky, T. C.; J.Toner, *Phys. Rev. Lett.* **1999**, *83*, 2745–2748.
- (25) Salditt, T.; Koltover, I.; Rädler, J. O.; Safinya, C. R. *Phys. Rev. Lett.* **1997**, *79*, 2582–2585.
- (26) Podgornik, R.; Zeks, B. *Phys. Rev. Lett.* **1998**, *80*, 305–308.
- (27) Schiessel, H. *Eur. Phys. J. B* **1998**, *6*, 373–380.
- (28) Schiessel, H.; Aranda-Espinoza, H. *Eur. Phys. J. E* **2001**, *5*, 499–506.
- (29) Andelman, D. Electrostatic properties of membranes: The Poisson–Boltzmann theory. In *Structure and Dynamics of Membranes*, 2nd ed.; Lipowsky, R., Sackmann, E., Eds.; Elsevier: Amsterdam, 1995; Vol. 1.
- (30) May, S.; Ben-Shaul, A. *J. Chem. Phys.* **1995**, *103*, 3839–3848.
- (31) Andelman, D.; Kozlov, M. M.; Helfrich, W. *Europhys. Lett.* **1994**, *25*, 231–236.
- (32) Carnie, S. L.; Chan, D. Y. C.; Stankovich, J. *J. Colloid Interface Sci.* **1994**, *165*, 116–128.
- (33) Stankovich, J.; Carnie, S. L. *Langmuir* **1996**, *12*, 1453–1461.
- (34) Houstis, E. N.; Mitchell, W. F.; Rice, J. R. *ACM Trans. Math. Software* **1985**, *11*, 379–418.
- (35) Sornette, D.; Ostrowsky, N. Lamellar Phases: Effect of fluctuations (Theory). In *Micelles, Membranes, Microemulsions and Monolayers*; Gelbart, W. M., Ben-Shaul, A., Roux, D., Eds.; Springer-Verlag: New York, 1994.
- (36) Helfrich, W.; Servuss, R. M. *Il Nuovo Cimento* **1984**, *3D*, 137–151.
- (37) Gawrisch, K.; Parsegian, V. A.; Hajduk, D. A.; Tate, M. W.; Gruner, S. M.; Fuller, N. L.; Rand, R. P. *Biochemistry* **1992**, *31*, 2856–2864.
- (38) Kozlov, M. M.; Leikin, S.; Rand, R. P. *Biophys. J.* **1994**, *67*, 1603–1611.
- (39) Chen, Z.; Rand, R. P. *Biophys. J.* **1997**, *73*, 267–276.